
(T4-fMRI) Using fMRI to Diagnose Schizophrenia

Farhad Haqiqat

Department of Computing Science
University of Alberta
haqiqath@ualberta.ca

Neil Borle

Department of Computing Science
University of Alberta
nborle@ualberta.ca

Shashindra Silva

Department of Electrical and Computer Engineering
University of Alberta
jayamuni@ualberta.ca

Abstract

Diagnosing schizophrenia is a challenging task for which diagnostic tests have yet to be developed, but where Functional Magnetic Resonance Imaging (fMRI) generated data is becoming increasingly available. fMRI has been used in conjunction with Sparse Gaussian Markov Random Field (SGMRF) to achieve high accuracy when diagnosing schizophrenia, however, these studies were limited by fairly small datasets that originated from single locations. In this work we focus on obtaining high diagnostic accuracies for data that has been combined from multiple locations. We evaluated the performance of two main approaches. First, we used SGMRF classifiers on voxel degrees extracted from fMRI data. Second, we used Regions of Interest (ROI) defined by Power *et al.* to extract a feature set from the data for learning and classification. After 5 repetitions of creating and evaluating on a balanced hold-out set where each location was represented equally, we found that an ROI approach used in conjunction with a SGMRF classifier provided the highest average accuracy (74.16%) on our multi-site data. While these accuracies are low in comparison to those obtain from single site analysis, we show that reasonable accuracies can be obtain when combining multiple schizophrenia datasets.

1 Introduction

Schizophrenia is a mental/psychiatric disorder [19, 11] known to affect blood flow in the brain [11] where those who are affected can experience hallucinations, delusions and diminished mental capacities to varying extents [10]. While several features of schizophrenia have proven useful for its diagnosis there are currently no set of features that have sufficient sensitivity or specificity to be used in diagnostic tests [10, 15]. This effectively means that subjectivity plays a role when a physician is diagnosing a patient.

Functional Magnetic Resonance Imaging (fMRI) is a tool for mapping of the functioning human brain caused by underlying brain electrical activity [14]. When a person is doing a task, neuron activity triggers increased blood flow to supply the neurons with the required glucose and oxygen[14]. Increased blood flow also brings more oxygen through blood vessels. The change in the level of oxyhemoglobin and deoxyhemoglobin (oxygenated or deoxygenated blood) changes the magnetic susceptibility of blood (BOLD signal) which is detectable through fMRI [14].

fMRI plays an important role in modern psychiatry research, as it provides the needed tool to determine dissimilarities in brain system that is a root for psychiatric illness[25]. An advantage of fMRI

is that it is non-invasive meaning that unlike some other imaging methods, no instruments or dyes are placed in the patients body [14, 7].

One of the tools used for studying schizophrenia is the Sparse Gaussian Markov Random Field (SGMRF) [19][22]. The primary advantage of using a SGMRF is that it has the ability to capture inter-voxel relationships that other methods cannot [19]. The resulting relationships can be used to observe differences in functional connectivity in the brain, allowing healthy subjects to be differentiated from schizophrenic subjects. Automated approaches to schizophrenia diagnosis have yielded accuracies of 93% for data that originates from a single location [19] and up to approximately 80% for data that originates from multiple locations [4].

In this work we consider probabilistic graphical models (PGMs) as a means of capturing differences in the interconnections between the brains of healthy patients and the brains of schizophrenics. We compare several different methods including those that use voxel degrees, regions of interest, Markov network structure and several other features.

2 Background and Prior Work

2.1 Regions of Interest and Single-Voxel Analysis

There are two main approaches for extracting information from fMRI images. The first is a single-voxel approach and the second is to study regions of interest (ROI) [8]. The trade-off between these two approaches is that a single-voxel approach requires the analysis of every voxel and is subject to the low signal-to-noise ratios of individual voxels, whereas a region based approach is only effective if the selected regions capture all relevant information in an fMRI task [8]. In 2011, Power *et al.* identified 264 putative function regions of interest derived from resting state fMRI, where no specific task is performed during data collection [17]. JD Power argues that these regions are currently the best available representation of the functional networks in the brain [17]. Several of the approaches used in this study directly build upon these regions.

2.1.1 Calculating Voxel Degrees

Introduced as a “degree map” in Rish *et al.* [21], voxel degrees are the constituent components of degree maps and are a feature of fMRI data that has been successfully used in schizophrenia diagnosis [19]. Voxel degrees represent the connectedness of voxels in the brain with the other voxels and are described as “the number of voxel neighbours in a network” [19]. Degrees are calculated in the following steps: First, multiple pair-wise Pearson correlation comparisons between all voxels to create a correlation matrix. Second, a threshold is applied to the correlation matrix. If a correlation value is greater than the threshold there said to be an edge between those two voxels. Finally, all of the edges in which a voxel participates are summed and the total number of edges becomes the degree of that voxel. Voxel degrees are used in several of our study’s approaches.

2.2 Rish *et al.*

Rish *et al.* [19] was able to achieve very high accuracies when diagnosing schizophrenia using fMRI data from a single location and employing several approaches. The most successful of these approaches include the use of support vector machines (SVM) and SGMRF classifiers, described later in the background. The error rate for SVM was 7% using pairwise correlation features, and 14% for the SGMRF using the 100 most significant voxels in the degree map feature set. We use the SGMRF approach described by Rish *et al.* [19]. In the MRF classifier, first they split training data in two different groups. For each group they compute the precision matrix (assuming the data is centered unless μ needs to be computed as well). See the *Inference* section of the Appendix for how they classify each new subject based parameters obtained from training stage.

2.3 Rosa *et al.*

Work by Rosa *et al.* [22] studied methods for diagnosing major depressive disorder (MDD). They used fMRI datasets and applied a SGMRF method to obtain the precision matrix. They then use an SVM on the precision matrix for the classification task. They obtained 85% accuracy on their first

dataset and 78.95% on their second dataset using this method. Both datasets were obtained using a single machine in a single location. The first dataset included 19 patients and 19 controls, and their second dataset included 30 patients and 30 controls. They also used SVM on the correlation feature, partial correlation and non sparse precision matrix to show effectiveness of their approach. Obtained accuracies were 68% 53% and 45% respectively, which are all worse than sparse precision matrix. Their approach can be compared to our approach in the *Individual MRF structure classification section*.

2.4 Multi-site Comparisons

Although, there were several prior work on the classification of schizophrenia patients using fMRI, most are based on data from a single site. Classification from multi-site data is inherently difficult due to the batch effects resulting from the use of different machines and environments. At the same time, multi-site analysis can easily be generalized for a new data set from a totally different source. Cheng et al. [4] analyzes a multi site data set which is obtained from five different sites with different machines. They used SVM to classify schizophrenia patients and healthy controls, and obtained accuracies are in the range of 73.53 – 80.92%. In this research we will try to obtain results with similar accuracies, but using PGM.

2.5 Principal Component Analysis

Principal Component Analysis (PCA) is a technique which uses mathematical techniques to transform data from an original space to a new dimensionality called principal components, which usually have smaller dimension than the original space. PCA uses vector space transformation to increase the dimensionality of large datasets. For doing so PCA uses mathematical projection [18].

The way PCA does this projection is by maximizing the variance of projected data. As Bishop [2] shows, if we project the data on the eigenvector(s) of the data variance will be maximum. Hence, if we want to project our N -dimensional data to the M -dimensional space where $M < N$, "the optimal linear projection for which the variance of the projected data is maximized is now defined by the M eigenvectors u_1, \dots, u_M of the data covariance matrix S corresponding to the M largest eigenvalues $\lambda_1, \dots, \lambda_M$." [2]: S and μ (the sample set mean) are defined as:

$$S = \frac{1}{N} \sum_{n=1}^N (X_n - \mu)(X_n - \mu)^T \quad (1)$$

$$\mu = \frac{1}{N} \sum_{n=1}^N X_n \quad (2)$$

2.6 Support Vector Machines

Vapnik *et al.* introduced the concept of support Vector Machines (SVMs) as a statistical tool for classification problems [23]. We use the most simple SVM, a linear SVM, because it does not use non-linear kernels and therefore has no hyperparameters that need to be tuned with cross validation. Instead, a linear SVM learns the "maximum-margin hyperplane" classifier which is a linear combination of the input features and partitions the data space into separate classes. The term "maximum-margin" refers to the SVM's ability to find the maximal separation between classes and the hyperplane, therefore creating the largest "margin" [23]. We can be guaranteed of the optimality of the result as the SVM problem is known to be convex [3]. The most simple form of a linear SVM minimizes $\frac{1}{2}||w||^2$ subject to the constraint $y_i(x_i w + b) - 1 \geq 0, \forall i$ where w is the weight vector, x_i is the instance's features, y_i is the instance label and b is the bias term of the model. Unfortunately, this version of the SVM only works in cases where the data is linearly separable. To extend the SVM to linearly inseparable data, the addition of positive slack variables is required, such that the constraints become $\forall i y_i(x_i w + b) - 1 + \xi_i \geq 0$ and $\xi_i \geq 0$, where ξ_i is the slack variable for the instance i [3].

2.7 Sparse Gaussian Markove Random Field (SGMRF)

One variation of Markov Random Field (MRF) is Gaussian MRF which is used for continuous space of variables and has well-defined mathematical properties that can be computed. Multivariate Gaussian density function over a set of random variables X is defined as below:

$$p(X) = (2\pi)^{-n/2} |\Sigma|^{-1/2} \exp \left\{ -\frac{1}{2} (X - \mu)^t \Sigma^{-1} (X - \mu) \right\}. \quad (3)$$

In the equation μ is the mean and Σ is the covariance matrix. We can set μ to zero and replace Σ^{-1} with C the equation (3) which can be written as the following form. It should also be noted that $C = \Sigma^{-1}$ and is known as the precision matrix in the literature.

$$p(X) = (2\pi)^{-n/2} |C|^{1/2} \exp \left\{ -\frac{1}{2} X^t C X \right\}. \quad (4)$$

It has been shown by Lauritzen [12] that X_i and X_j are independent if and only if their corresponding entries in the precision matrix (C) are zero. It can be concluded that missing edge in the MRF will lead to zero entries in the precision matrix [20]. The problem of learning pgm for a given dataset is reduced to learning the precision matrix given this proof.

The log-likelihood of the dataset, assuming each row of the data is a p -dimensional vector and consisting n samples $D = \{X_1, X_2, \dots, X_n\}$, can be written as follow. It should also be noted that we assume each sample is identically independent distributed (iid).

$$L(D) = \frac{n}{2} \ln |C| - \frac{1}{2} \sum_{i=1}^n (X_i - \mu)^T C (X_i - \mu) + \text{const}, \quad (5)$$

Here, const is a constant which is not dependent on μ or C . We can also center the data in such a way that $\mu = 0$, so the second term reduces to $\frac{1}{2} \sum_{i=1}^n X_i^T C X_i$ which is equal to $\frac{n}{2} \text{tr}(AC)$, where tr is trace of the matrix. The above formula can be written as shown in equation (6) where the log-likelihood maximization problem is shown in equation (7).

$$L(D) = \frac{n}{2} [\ln |C| - \text{tr}(AC)] + \text{const} \quad (6) \quad \max_{C \succ 0} |C| - \text{tr}(AC) \quad (7)$$

Here $|\dots|$ represents determinant and A is the empirical covariance matrix calculated by $A = \frac{n}{2} \sum_{i=1}^n X_i^T X_i$, or maximum likelihood estimation for Σ . It should also be noted the $C \succ 0$ constraint makes C positive definite.

To achieve sparse formulation for Gaussian Markov Random Field we can use the Laplace prior. If we impose the Laplace prior on the precision matrix $p(C_{ij}) = \frac{\lambda_{ij}}{2} e^{-\lambda_{ij} |C_{ij}|}$ we can achieve sparsity. This will change the equations (6) and (7) to the following forms below where the l_1 -norm of C is $\|C\|_1 = \sum_{i,j} C_{ij}$, and $\rho = \frac{n}{2} \lambda$.

$$L(D) = \frac{n}{2} [\ln |C| - \text{tr}(AC)] - \lambda \|C\|_1, \quad (8) \quad \max_{C \succ 0} \ln |C| - \text{tr}(AC) - \rho \|C\|_1, \quad (9)$$

2.7.1 Method for obtaining precision matrix

One obvious way for learning the parameters for joint distribution probability is using regularized likelihood maximization such as Akaike information criterion (AIC) and Bayesian information criterion (BIC). However, finding the simplest model which fits the data is a NP-hard problem

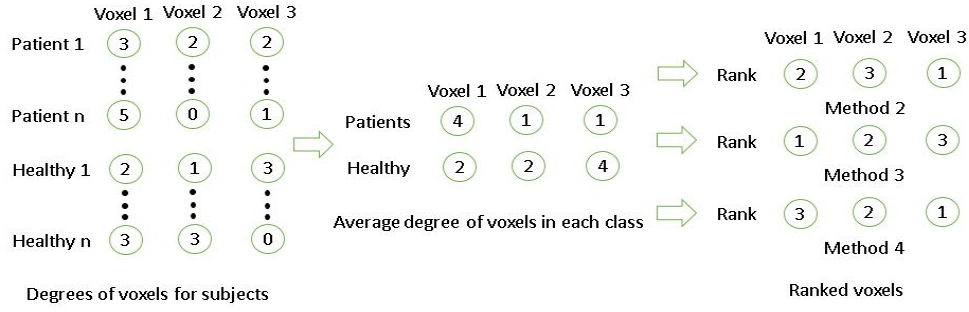


Figure 1: Voxel ranking methods to select best voxels. In step 2, the differences of the average degrees between patients and healthy subjects are 2, -1, and -3 respectively for the three voxels.

using this approach. There are also few limitations that make using this approach less desirable. First Empirical covariance matrix may not even exist, specially when the number of features in the dataset is more than the number of samples. Which is the case in fMRI studies. fMRI datasets usually have fraction of samples to features. Second problem using this approach is not having zero elements in the inverse of empirical covariance matrix. Hence, to construct the MRF using this matrix one should include explicit sparsity constraint [20].

These two major problems cause us to search for other solution to build the precision matrix given the dataset. Fortunately one can use the alternative approximation approach for the above problem. Recently there have been some successes for getting the approximate precision matrix given the dataset. Glasso[6], block-coordinate descend (BCD) known as COVSEL [1], Varsel [9] and projected gradient [13] approach are among them. For further reading on these methods readers can refer to [20]. In this study we are using Varsel and glasso as the preferred method for obtaining the precision matrix and subsequently MRF.

3 Methodology

3.1 Data Set

Data used for this study were downloaded from the Function BIRN Data Repository (<http://fbirnldr.birncommunity.org:8080/BDR/>). The original data contained nine sites and 235 subjects. However, during the preprocessing steps some of the subjects were removed because they could not be preprocessed properly, resulting in a final set of 95 subjects and five sites. Data were pre-processed by Dr. Mina Gheiratmand by using FSL software (<http://fsl.fmrib.ox.ac.uk/fsl/fslwiki/>). Our data contained 46 schizophrenic subjects and 49 healthy subjects. Each subject had four runs (repeated scans) so effectively our data set consists of 380 subjects. Each run had 137 time slices and each time slice had the signal amplitude of over 100,000 voxels. The voxels were referred using the 3D coordinates and thus the dimensionality of a single run was $\mathcal{R}^{53 \times 64 \times 37 \times 137}$. We removed 80% of subjects from each site as our holdout set and used the remaining set as our training set. Furthermore, we made sure that the holdout set was also balanced, so that the ratio between the patients and healthy subjects was same in the holdout and training sets for each site. We made sure that all the runs from the same subject either belonged to the holdout set or to the training set. The training set was used for finding the hyper-parameters of the system using five-fold cross validations. After finding the hyper parameters we used the full training set to train the system with the selected hyper parameter and obtained the accuracy of the hold out set. We repeated this procedure five times for different hold out sets to get an average accuracy.

3.2 SGMRF with log degrees of ranked voxels

First, we executed the approach proposed by Rish *et al.* [19] on our data set. We had degrees of each voxels as well as the smoothed log values of the voxels for each subject. Furthermore, as

some voxels of some subjects had zero values for the BOLD signal, an universal mask was used to select the voxels which had a non-zero BOLD signal value through the whole data set. This resulted in a 28719 voxels per each subject. However, using all the available voxels resulted in significantly increased computation time and thus selecting the best voxels (based on the training data) to separate the healthy and schizophrenic subjects was very important.

To select the best voxels out of the possible 28719 voxels, we experimented with multiple approaches. These included selecting voxels based on t-tests (method 1), based on absolute differences of mean voxel degrees (method 2), based on differences of mean voxel degrees (method 3) (*schizophrenic* – *healthy*) and based on differences of mean voxel degrees (method 4) (*healthy* – *schizophrenic*).

The last three voxel ranking methods are explained in Figure 1. Out of the above four approaches we obtained the highest accuracy on our cross validation set by the third approach. Also the number of voxels k to be used in the SGMRF model was decided by running the experiment for different k values and finding that $k = 20$ performed well during cross validation. By using the selected voxels, we obtained the precision matrices for schizophrenic and healthy subjects. Similar to the value of k , the sparsity coefficient λ was also obtained through a hyper parameter search on our cross validation set.

3.3 SGMRF with degrees from Dorsolateral Prefrontal Cortex area

Different studies have shown that connections in certain areas of the brain specifically dorsolateral prefrontal cortex (DLPFC) [16] and thalamocortical [4] circuitry changes for schizophrenic patients. Thus, we extracted the degrees of voxels in these areas and used them to build the SGMRF model. Since we had only 4504 voxels for each subject, we did not perform any voxel rankings in this approach. Similar to the previous approach using the smoothed log values of the degrees resulted in higher accuracy.

3.4 Methods using Power *et al.*'s ROIs

The following three methods used in this subsection all involve the 264 regions of interest that are described in work by Power *et al.* [17]. Due to missing data resulting from incomplete scans of subjects, 8 regions were removed from analysis leaving 256 ROIs. See appendix for list of omitted region coordinates. We use the approach described by Vega *et al.* [24] to summarize regions of interest by taking region averages for each of the 5mm radius spheres that define regions. Finally this resulted in a 137×256 matrix for each subject where each row is a time point across all regions and each column is the average time series for a single region. The permitted SGMRF hyperparameter λ values were 0.7, 0.1, 0.07, 0.01 and 0.007 for this section.

3.4.1 ROI with Subject Concatenation

For this approach we follow the method described by Vega *et al.* [24]. Training set subjects in each class are first concatenated so that two large matrices are created, one with dimension $ns * 137 \times 256$ and the other with dimension $nh * 137 \times 256$ where ns is the number of schizophrenic subjects in the training set and nh is the number of healthy subjects. To make learning the SGMRF structure faster we also used the same feature normalization as was described by Vega *et al.* [24], where for each class and each region in that class the region mean was subtracted from each time point and each time point was divided by the region standard deviation. Next, with the use of Glasso, a SGMRF structure was learned for each class which resulted in two sparse precision matrices that encode the independences learned. Finally, when presented with a new subject from the hold-out set, equations (8) and (9) were used to determine the likelihood of the subject belonging to each class followed by which class the new subject should be assigned.

A modified version of this approach was also implemented and tested but has been omitted for brevity and due to it obtaining poor results. See appendix for background information. In this variant, a Fourier transform was used on each of the subject's time series data to obtain Fourier coefficients. These Fourier coefficients were then used in place of the original time series for learning a classifier.

3.4.2 Region Degrees

Like the work described in Rish *et al.* [21], region degrees are also used in this approach but in this case, we only considered the degrees that result from the 256 ROIs. This process is illustrated in Figure 2. The only difference in the process described previously is that we explicitly remove the self correlations in the correlation matrix (the diagonal), and we conceptually represent the process as binarizing a matrix and summing over its rows. We also chose to use a threshold value of 0.7 as was done in Rish *et al.* [21].

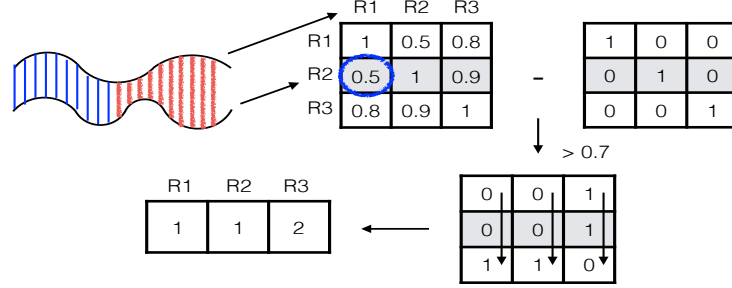


Figure 2: Pair-wise comparisons are made between region time series data to produce a correlation matrix. The diagonal is removed and a threshold is applied to binarize the matrix. Sums are collected for each region to produce the “degree” of that region.

Now that we had a vector of region degrees (1×256) for each subject, a SGMRF was used to again to build a classifier. This followed similarly from the previous approach except that now the input to Glasso was a $ns \times 256$ matrix for schizophrenic patients and a $nh \times 256$ matrix for healthy subjects. Again this resulted in two 256×256 precision matrices which we could use in likelihood calculations for subjects from the hold-out set. Additionally, we also used a linear SVM classifier trained directly on region degree data to compare its performance to the SGMRF classifier.

3.4.3 Individual MRF Structure Classification

This approach is similar to the region concatenation approach described previously except that here we did not concatenate subjects and instead learned a precision matrix (SGMRF structure) for each subject individually. For example, if we had ns_{total} schizophrenics in our dataset and nh_{total} healthy subjects ($ns_{total} + nh_{total}$ 137×256 matrices) then we would use Glasso to generate $ns + nh$ precision matrices.

To build a classifier, a linear SVM is trained on the precision matrices generated from the training set and then tested on the precision matrices generated from the hold-out set.

3.5 Other Features Including PCA

We have tried different features using the approach proposed by Rish *et al.*. Features that are used for this approach are as following: [Correlation , Log-Disconnection, Log-Disconnection Regions, Eignevalues, MBI stat, Degree]. This features were provided to us with the dataset. So we wanted to see how good results would be implementing the exact same approach as suggested by Rish *et al.*. In this experiment we first selected the hyper parameters; number of features and λ ; using 5-fold cross validation and then test those parameters on the hold-out set. The hold-out set has been selected randomly from different site with criteria of being balanced with regards to healthy and schizophrenic, and according to the ratio of each group’s subjects in each site. Result that we achieved had accuracy of less than 50% for all features except than degrees and disconnection which achieved 65.55% and 63.33% accuracy respectively.

Another approach that we have used for feature selection was using PCA for transforming the dataset to lower dimension. We hoped this could magnify distinguishing features in the dataset while reducing it size. Unfortunately results were not as we hoped and were mostly near the chance level. It should be mentioned that we chose three different sizes for the number of principal components that we used :3, 35 and 70.

4 Results and Discussion

	Rish (Full)	Rish (DLPFC)	ROI + Concatenation	Region Degrees	MRF structure	Other Features
Classifier	SGMRF	SGMRF	SGMRF	SVM	SVM	SGMRF
Accuracy	72.32%	63.52%	74.17%	60.65%	69.44%	65.55%

Table 1: Accuracy on 5 Striated Hold-out Sets

As Seen in Table 1 methods using a SGMRF classifier were able to obtain the best results, of which 74.17% was the highest average accuracy recorded. This seems to suggest that a SGMRF seems to be a more effective tool for this particular problem. A possible explanation for the success of the SGMRF approach when using ROI and concatenating patient data might be the results of reduced feature set size and increased input data size for training. When comparing Rish (Full/DLPFC) in Table 1 to the ROI + Concatenation approach, the Rish approaches use voxels as their features whereas ROI + Concatenation only uses 256 regions of interest as features. Given that our dataset only consists of 380 examples, there is a much larger gap (28719 features for Full and 4504 features for DLPFC) in number of features compared to number of training examples for these Rish approaches. Further, because each time point in the ROI + Concatenation approach is considered as a sample from the region of interest, this approach has 137 times as much input data when training as compared to all other methods used and it could be this that is boosting classification accuracy. Between the two Rish methods we can see that DLPFC performs significantly more poorly as compared to the other method which seems to suggest that the DLPFC region is not sufficient for capturing the differences between controls and schizophrenic patients. The region degrees approach also performed poorly. While it is not clear why it performed so poorly, it might be the case that voxel degree approaches need the full set of voxels to be effective. This would explain the decreasing accuracies as we reduce the number of features used where 28719, 4504 and 256 features correspond to Rish (Full), Rish (DLPFC) and Region degrees, the voxel degree approaches tested. The approach classifying subjects by the SGMRF structures learned performed surprisingly well which suggests that a graphical models structure could potentially be useful, in addition to maximum likelihood when diagnosing schizophrenia. Finally, while we considered many other features including PCA in our Other Features section, few performed well. The best of these was closely related to the Rish (Full) approach which indicated that voxel degrees have more discriminative power for this task as compared to many other features.

5 Conclusions and Future Work

In this work we studied the use of fMRI and machine learning to diagnose schizophrenia, given a set of healthy and schizophrenic subjects. We found that a region based approach using SGMRFs yielded the highest accuracy (74.16%) when averaged over 5 hold-out sets where the hold-out set was composed of 20% of each site used in the study. We conclude from this that ROIs are more effective in the diagnosis of schizophrenia than whole brain analysis because extraneous noise is being removed from the data and further, that representing your data in such a way to maximize the number of training examples seen is beneficial to this problem.

In this study we did not select the number of principal components based on the variance captured by the components, future work could be done to explore this method and determine if it could improve classification accuracy. Other future work involves the use of ensemble methods. We have found that several methods perform well individually, so an attempt at combining them together seems like a natural next step.

6 Acknowledgements

We would like to thank Dr. Mina Gheiratmand for preprocessing the fMRI data and co-coaching our project, Sugai Liang for her advice and Roberto Vega for all his advice and help. Finally, we would also like to thank Dr. Irina Rish for the feature extraction code she provided and Dr. Greiner for his supervision of this project.

References

- [1] Onureena Banerjee, Laurent El Ghaoui, and Alexandre d’Aspremont. Model selection through sparse maximum likelihood estimation for multivariate gaussian or binary data. *J. Mach. Learn. Res.*, 9:485–516, June 2008.
- [2] Christopher M Bishop. Pattern recognition. *Machine Learning*, 2006.
- [3] Christopher JC Burges. A tutorial on support vector machines for pattern recognition. *Data mining and knowledge discovery*, 2(2):121–167, 1998.
- [4] Wei Cheng, Lena Palaniyappan, Mingli Li, Keith M Kendrick, Jie Zhang, Qiang Luo, Zening Liu, Rongjun Yu, Wei Deng, Qiang Wang, Xiaohong Ma, Wanjun Guo, Susan Francis, Peter Liddle, Andrew R Mayer, Gunter Schumann, Tao Li, and Jianfeng Feng. Voxel-based, brain-wide association study of aberrant functional connectivity in schizophrenia implicates thalamocortical circuitry. *Npj Schizophrenia*, 1, May 2015.
- [5] Pierre Duhamel and Martin Vetterli. Fast fourier transforms: a tutorial review and a state of the art. *Signal processing*, 19(4):259–299, 1990.
- [6] Jerome Friedman, Trevor Hastie, and Robert Tibshirani. Graphical lasso in r and matlab.
- [7] Amiram Grinvald, Hamutal Slovin, and Ivo Vanzetta. Non-invasive visualization of cortical columns by fMRI. *Nature Neuroscience*, 3(2):105–107, feb 2000.
- [8] Ruth Heller, Damian Stanley, Daniel Yekutieli, Nava Rubin, and Yoav Benjamini. Cluster-based analysis of fmri data. *NeuroImage*, 33(2):599–608, 2006.
- [9] Jean Honorio, Dimitris Samaras, Nikos Paragios, Rita Goldstein, and Luis E Ortiz. Sparse and locally constant gaussian graphical models. In *Advances in Neural Information Processing Systems*, pages 745–753, 2009.
- [10] Assen Jablensky. The diagnostic concept of schizophrenia: its history, evolution, and future prospects. *Dialogues Clin Neurosci*, 12(3):271–287, 2010.
- [11] Nomura Kenji. Pressure-induced performance decrement in verbal fluency task through pre-frontal overactivation: A near-infrared spectroscopy study. *Front. Neurosci.*, 4, 2010.
- [12] S.L. Lauritzen. *Graphical Models*. Oxford Statistical Science Series. Clarendon Press, 1996.
- [13] Yuanqing Lin, Shenghuo Zhu, Daniel D Lee, and Ben Taskar. Learning sparse markov network structure via ensemble-of-trees models. In *International Conference on Artificial Intelligence and Statistics*, pages 360–367, 2009.
- [14] PM Matthews and P Jeppard. Functional magnetic resonance imaging. *Journal of Neurology, Neurosurgery & Psychiatry*, 75(1):6–12, 2004.
- [15] Philip McGuire, Oliver D Howes, James Stone, and Paolo Fusar-Poli. Functional neuroimaging in schizophrenia: diagnosis and drug discovery. *Trends in Pharmacological Sciences*, 29(2):91 – 98, 2008.
- [16] S G Potkin, J A Turner, G G Brown, G McCarthy, D N Greve, G H Glover, D S Manoach, A Belger, M Diaz, C G Wible, J M Ford, D H Mathalon, R Gollub, J Lauriello, D O’Leary, T G M van Erp, A W Toga, A Preda, K O Lim, and FBIRN. Working memory and DLPFC inefficiency in schizophrenia: The FBIRN study. *Schizophrenia Bulletin*, 35(1):19–31, November 2008.
- [17] Jonathan D. Power, Alexander L. Cohen, Steven M. Nelson, Gagan S. Wig, Kelly Anne Barnes, Jessica A. Church, Alecia C. Vogel, Timothy O. Laumann, Fran M. Miezin, Bradley L. Schlaggar, and Steven E. Petersen. Functional network organization of the human brain. *Neuron*, 72(4):665–678, nov 2011.
- [18] Mark Richardson. Principal component analysis. URL: <http://people.maths.ox.ac.uk/richardsonm/SignalProcPCA.pdf> (last access: 3.5. 2013). Aleš Hladnik Dr., Ass. Prof., Chair of Information and Graphic Arts Technology, Faculty of Natural Sciences and Engineering, University of Ljubljana, Slovenia ales.hladnik@ntf.uni-lj.si, 2009.
- [19] Irina Rish, Guillermo Cecchi, Benjamin Thyreau, Bertrand Thirion, Marion Plaze, Marie Laure Paillere-Martinot, Catherine Martelli, Jean-Luc Martinot, and Jean-Baptiste Poline. Schizophrenia as a network disease: Disruption of emergent brain function in patients with auditory hallucinations. *PLoS ONE*, 8(1):e50625, jan 2013.

- [20] Irina Rish and Genady Grabarnik. *Sparse Modeling: Theory, Algorithms, and Applications*. CRC Press, Inc., Boca Raton, FL, USA, 1st edition, 2014.
- [21] Irina Rish, Benjamin Thyreau, Bertrand Thirion, Marion Plaze, Marie-laure Paillere-martinot, Catherine Martelli, Jean-luc Martinot, Jean-Baptiste Poline, and Guillermo A Cecchi. Discriminative network models of schizophrenia. In *Advances in Neural Information Processing Systems*, pages 252–260, 2009.
- [22] Maria J. Rosa, Liana Portugal, John Shawe-Taylor, and Janaina Mourao-Miranda. Sparse network-based models for patient classification using fMRI. In *2013 International Workshop on Pattern Recognition in Neuroimaging*. Institute of Electrical & Electronics Engineers (IEEE), jun 2013.
- [23] Armin Shmilogici. Support vector machines. In *Data Mining and Knowledge Discovery Handbook*, pages 257–276. Springer, 2005.
- [24] Roberto Vega, Khare Kriti, and Sayem Mohammad Siam. Gender and age group classification using functional magnetic resonance imaging and gaussian markov random fields. *Unpublished*, 2015.
- [25] Xiaoyan Zhan and Rongjun Yu. A window into the brain: Advances in psychiatric fMRI. *BioMed Research International*, 2015:1–12, 2015.

7 Appendix

7.1 Fourier Transform

A Fourier transform allows for the translation of any signal from the time domain to the frequency domain. More specifically, it takes a signal and decomposes it into a series constituent sin and cos componets. When taking the Fast Fourier Transform or FFT of real data the resulting peaks in the frequency domain are conjugate symmetric [5], meaning that methods that only require the real component of the data need only work with half of the resulting component coefficients in the transform. These Fourier coefficients can be used in place of the original signal as features provided to a machine learning classifier.

7.2 Omitted ROI coordinates

The regions removed are characterized by region number with the associated MNI coordinates described in Power *et al.* provided in parenthesis: 81 (-44, 12, -34), 82 (46, 16, -30), 128 (52, 7, -30), 184 (17, -80, -34), 247 (33, 12, -34), 248 (-31, -10, -36), 249 (49, -3, -38) and 250 (-50, -7, -39).

7.3 Inference

Once we have constructed probabilistic graphical model through precision matrix we can use that to do probabilistic inference for variables of interest. To make it more clear let assume X is our dataset and $Z \subset X$ is the subset of our dataset which is observed with assigned values of z , and let $Y \subseteq X - Z$ be the set of unobserved variables. Now we can use inference to compute posterior probability of $P(Y|Z = z)$. In this task Y is a binary variable, and classification task is to find the assignment for y which makes the $P(Y|Z = z)$ maximum. $y^* = \operatorname{argmax}_y P(Y = y|Z = z)$. Bayes rule give us:

$$P(Y = y|Z = z) = \frac{P(Z = z|Y = y)P(Y = y)}{P(Z = z)} \quad (10)$$

And since denominator is fixed for each assignment $Y=y$. We compute the *argmax* only using the numerator.

$$y^* = \operatorname{argmax}_y P(Z = z|Y = y)P(Y = y) \quad (11)$$

So for a given dataset we can learn the model $P(Z = z|Y = y)P(Y = y)$ for each class label, and then given a test dataset assign the most likely class label using the equation(11) [20]

7.4 Description of the features

1. Correlation: All pair-wise correlations between super-voxels in the (spatially) down-sampled data. The original data is $53 \times 64 \times 37$ voxels. The number of all pair-wise correlations is extremely large for the original data. Data have been down sampled to $13 \times 16 \times 12$. Then all of the pair-wise correlations computed, which is $(731 \times 731 - 731)/2$. 731 is the number of nonzero elements in the subjects universal brain mask (intersection of all subjects brains) in the down sampled data.
2. Eigenvalues: (Nonzero) eigenvalues of the correlation matrix
3. Log-disconnection: instead of thresholding for correlation coefficient $r > 0.7$ and finding the degrees, It has been thresholded for $r < 0.4$ to have a measure of dis-connectivity of a voxel. In contrast, with the degree features.
4. Log-disconnection regions: as the log-disconnection feature, but with only difference of being limited to three regions: superior frontal gyrus, middle frontal gyrus and Thalamus.
5. MBI stat: statistics of the average brain intensity signal (for each subject) as the feature. These were mean, standard deviation, skewness and Kurtosis.
6. Degree: as described in the report.